Bergische Universität Wuppertal

Fachbereich Mathematik und Naturwissenschaften

Institute of Mathematical Modelling, Analysis and
Computational Mathematics (IMACM)

Preprint BUW-IMACM 15/33

Poitr Putek, Kai Gausling, Andreas Bartel,
Konstanty M. Gawrylczyk, Jan ter Maten, Roland Pulch,
Michael Günther

Robust topology optimization of a permanent magnet synchronous machine using multi-level set and stochastic collocation methods

October 2015

http://www.math.uni-wuppertal.de

Robust topology optimization of a permanent magnet synchronous machine using multi-level set and stochastic collocation methods

Piotr Putek[1,3], Kai Gausling[1], Andreas Bartel[1], Konstanty M. Gawrylczyk[2], Jan ter Maten[1], Roland Pulch[3], and Michael Günther[1]

Abstract The aim of this paper is to incorporate the stochastic collocation method (SCM) into a topology optimization for a permanent magnet (PM) synchronous machine with material uncertainties. The variations of the non-/linear material characteristics are modeled by the Polynomial Chaos Expansion (PCE) method. During the iterative optimization process, the shapes of rotor poles, represented by zero-level sets, are simultaneously optimized by redistributing the iron and magnet material over the design domain. The gradient directions of the multi-objective function with constraints, composed of the mean and the standard deviation, is evaluated by utilizing the continuous design sensitivity analysis (CDSA) with the SCM. Incorporating the SCM into the level set method yields designs by using already existing deterministic solvers. Finally, a two-dimensional numerical result demonstrates that the proposed method is robust and effective.

1 Introduction

Nowadays, permanent-magnet (PM) machines have become more popular due to their attractive features such as a high performance, efficiency, and power density [2]. Therefore, they have found a broad use in industrial applications such as robotics, computer peripherals, industrial drivers or automotive industry, for example, in commercialized hybrid vehicles with different hybridization level, e.g. [3, 5]. However, this type of motor construction suffers inherently from a relatively high level of acoustic noise and mechanical vibration. In the case of a PM machine, the interaction between the stator slot driven air-gap performance harmonics and the

[1] University of Wuppertal, Chair of Applied Mathematics & Numerical Analysis, Germany, {putek,gausling,bartel,termaten,guenther}@math.uni-wuppertal.de ·
[2] West Pomeranian University of Technology, Department of Electrotechnology and Diagnostic, Szczecin, Poland, Konstanty.Gawrylczyk@zut.edu.pl ·
[3] Ernst-Moritz-Arndt-Universität Greifswald, Germany, pulchr@uni-greifswald.de.

magnet driven magnetomotive force (MMF) harmonics is mainly responsible for producing a high cogging torque (CT). On the other hand, the torque ripple developed in electromagnetic torque is caused by the cogging torque and harmonic contents in the back-electromotive force (EMF). In addition, magnetic saturations in the stator and rotor cores with the converted related issue may further disturb the electromagnetic torque of the machine [4]. Therefore, the designers aim above all at reducing the torque fluctuations. In turn, this may significantly affect the machine performance.

In this paper, we focus on optimizing the topology a PM machine, as the machine topology itself is a major contributor to the electromagnetic torque fluctuation. Because the result of the design procedure is strongly affected by the unknown material characteristics [6], the uncertainties in modeling the soft ferromagnetic material are taken into account. In some applications [7], especially the relative permeability of the magnetic material itself should be accounted to model more accurately the magnetic flux density of permanent magnets. This parameter is also in our model assumed as uncertain. The novel aspect of the proposed method is the incorporation of stochastic modeling into the topology optimization method for the low cogging torque (CT) design of an Electric Controlled Permanent Magnet Excited Synchronous Machine (ECPSM).

2 Model description

In the design of a PM machine, the shape/fabrication and the placement of magnets, iron poles and air-gaps primarily determine the torque characteristic. A part of an assembly drawing of such a device, considered as a case study in our paper, is given in Fig. 1. The structure of the rotor comprises two almost identical parts, which differ only in the magnetization direction of the constructed PM poles of the rotor. The key feature of the machine is the installation of an additional DC control coil that is fixed in the axial center of the machine, between two laminated stators. The proper supply of this coil by the DC-chopper enables to control the effective excitation of the machine. In the end, this results in a field weakening of 1:4, which is of great importance in electric vehicles applications. The magnetic behavior can be described in terms of the unknown magnetic vector potential (MVP) A for the quasi-linear curl-curl equation. In fact, in order to reduce the computational burden, we consider two dimensional (2-D) model that is additionally simplified by neglecting the eddy current phenomena, i.e., ($\sigma \frac{\partial A}{\partial t} = 0$). Then, the curl-curl equation becomes a Poisson equation

$$\nabla \cdot \left(\upsilon(\mathbf{x}, |\nabla A(\mathbf{x})|^2) \nabla A(\mathbf{x}) - \upsilon_{\mathrm{PM}} \mathbf{M}(\mathbf{x}) \right) = J(\mathbf{x}), \quad \mathbf{x} \in \mathrm{D} \subset \mathbb{R}^2, \tag{1}$$

equipped with the periodic boundary condition Γ_{PBC} on $\partial \mathrm{D}$ in order to further decrease the computational burden. This establishes the computational domain D, cf. Fig. 3. Here, the current density is denoted by $J \in L^2(\mathrm{D})$ and the remanent flux

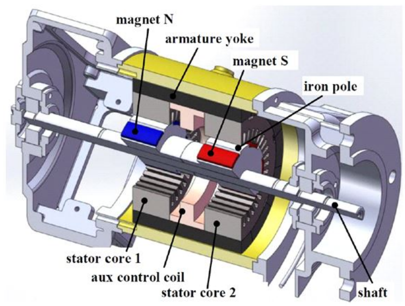

Table 1
Main parameters of the ECPSM topology

$2p$: number of poles	12
r_{ostat}: outer radius of the stator	67,5 mm
r_{istat}: inner radius of the stator	41,25 mm
l_{as}: axial length one part of the stator	35 mm
w_{oslot}: width of the slot opening	4,0mm
ns: number of slots	36
m: number of phases	3
t_m: thickness of magnets ($NdFeB, B_r$=1,2T)	3,0 mm

Fig. 1 Cross-section of an ECPSM and its main parameters (surface-mounted PM rotor, three-phase windings, fixed excitation control auxiliary coil) [5].

density of the PM is denoted by $\mathbf{M}$. Furthermore, the reluctivity υ is as a real parameter, which describes the isotropic material relation $\mathbf{H} = \upsilon(|\mathbf{B}|^2)\mathbf{B}$ between the flux density $\mathbf{B} = \nabla A$ and the field strength $\mathbf{H}$. The parameter υ depends on ∇A. In the air-gap, the vacuum reluctivity $\upsilon(|\mathbf{B}|^2) = \upsilon_0$ is taken into account. The quality of the design of a PM motor, on the one hand, is assessed by the cogging torque fluctuation T. This quantity is calculated by using the Maxwell stress tensor method [2]

$$T(\theta) = \upsilon_0 \oint_S \mathbf{r} \times \left((\mathbf{n} \cdot \mathbf{B}(\mathbf{x}))\mathbf{B}(\mathbf{x}) - \frac{|\mathbf{B}(\mathbf{x})|^2}{2}\mathbf{n} \right) \mathrm{d}S, \tag{2}$$

where $\mathbf{n}$ is unit outward normal vector and S denotes any closed integration surface in the air gap surrounding the rotor and $\mathbf{r}$ denotes the position vector. Its main contributor is the machine topology. Additionally in the bi-objective optimization problem, the root mean square (*rms*) value of the magnetic field density calculated in the air-gap along the path l is treated as the second criterion [15]

$$B^2_{\mathrm{r-rms}} = \frac{1}{L}\int_{\theta_1}^{\theta_2} |B_r|^2 \mathrm{d}l \geq \alpha, \tag{3}$$

where the coefficient α denotes an assumed level of the magnetic flux density in the air-gap (the fraction of $B_{\mathrm{r-rms}}$ calculated for the initial configuration), L refers to the length of the path l (from θ_1 to θ_2).

A further difficulty regards the reluctivty υ: it is discontinuous across material borders and it is nonlinear in ferromagnetic materials. Moreover, the ferromagnetic material characteristics (deduced from measurements) suffers from uncertainties [6]. In certain applications, especially the relative permeability of the magnetic material should be modeled to obtain a more accurate magnetic flux density of permanent magnets [7]. Since the uncertainties affect the results of the design procedure, we have to include these uncertainties to enable a robust design. That is, the reluctivity becomes a random variable. To this end, we consider the following parameters as uncertain $\boldsymbol{\upsilon} := \left(\upsilon_{\mathrm{PM}}, \upsilon_{\mathrm{Fe}}, \upsilon_{\mathrm{air-gap}}\right) := \mathbf{p}$ in the stochastic reluctivity model. The uncertainty of $\upsilon_{\text{air-gap}}$ is rather mathematical; it could account for inaccuracies of the gap or material inside the gap.

3 Stochastic forward problem

For uncertainty quantification, we replace the parameters $\boldsymbol{\upsilon} : \Omega \to \Pi \subset \mathbb{R}^3$ by independent random variables $\boldsymbol{\upsilon}(\boldsymbol{\xi})$ defined on some probabilistic space $(\Omega, \mathscr{F}, \mathbb{P})$ with a joint density $\rho : \Pi \to \mathbb{R}$. In our case, it will be a uniform distribution (ranging $\pm 10\%$ around the respective nominal values).[1] Consequently, the direct problem is governed by the random-dependent PDEs system

$$\begin{cases} \nabla \cdot \left(\upsilon_{\text{Fe}}\left(\mathbf{x}, |\nabla A(\mathbf{x})|^2, \xi_1\right) \nabla A(\mathbf{x})\right) = 0, & \text{in } \Omega_{\text{Fe}}, \\ \nabla \cdot \left(\upsilon_{\text{air-gap}}(\mathbf{x}, \xi_2) \nabla A(\mathbf{x})\right) = 0, & \text{in } \Omega_{\text{air}}, \\ \nabla \cdot (\upsilon_{\text{PM}}(\xi_3) \nabla A(\mathbf{x})) = \nabla \cdot \upsilon_{\text{PM}}(\xi_3) \mathbf{M}(\mathbf{x}), & \text{in } \Omega_{\text{PM}}, \end{cases} \tag{4}$$

where $A : \mathrm{D} \times \Omega \to \mathbb{R}$ with $\mathrm{D} = \Omega_{\text{air}} \cup \Omega_{\text{Fe}} \cup \Omega_{\text{PM}}$, becomes a random field. The statistical information like the expected value for a function $f : \Pi \to \mathbb{R}$ reads as

$$\langle f(\boldsymbol{\upsilon})\rangle := \mathbb{E}[f(\boldsymbol{\upsilon})] = \int_{\Pi} f(\boldsymbol{\upsilon})\rho(\boldsymbol{\upsilon})\,\mathrm{d}\boldsymbol{\upsilon}, \tag{5}$$

provided that the integral is finite. Furthermore, for two functions $f, g : \Pi \to \mathbb{R}$ this operator yields an inner product $\langle f, g\rangle := \mathbb{E}(f(\boldsymbol{\upsilon})g(\boldsymbol{\upsilon}))$ on $L^2(\Omega)$, see e.g. [8, 11]. If each component υ_i exhibits a finite second moment, then the random field A can be expanded in the truncated polynomial chaos (PC) series [11]

$$A(\mathbf{x}, \boldsymbol{\upsilon}) = \sum_{i=0}^{N} \mathrm{v}_i(\mathbf{x}) \Phi_i(\boldsymbol{\upsilon}) \tag{6}$$

with unknown a priori coefficient functions v_i. Here, the basis functions $(\Phi_i)_{i\in\mathbb{N}}$ with $\Phi_i : \Pi \to \mathbb{R}$ are orthonormal polynomials, i.e., $\langle \Phi_i(\boldsymbol{\upsilon}), \Phi_j(\boldsymbol{\upsilon})\rangle = \delta_{ij}$ with the Kronecker delta δ_{ij}. To calculate v_i the SCM with Stroud integration formula [9, 10] is used. The basic concept is to provide the solution of the deterministic problem at each quadrature grid point $\boldsymbol{\upsilon}^{(k)}$, $k = 0, \ldots, K$. The Stroud rules yield a relatively small number of grid points for a quadrature of a fixed order. Thus, finally we approximate statistical quantities like the mean and the standard deviation

$$\mathbb{E}[\mathrm{A}(\mathbf{x}, \boldsymbol{\upsilon})] = \mathrm{v}_0(\mathbf{x}), \quad \mathrm{std}[\mathrm{A}(\mathbf{x}, \boldsymbol{\upsilon})] = \sqrt{\sum_{\mathrm{i}=1}^{\mathrm{N}} |\mathrm{v}_{\mathrm{i}}(\mathbf{x})|^2} \tag{7}$$

[1] For the UQ, the stochastic reluctivity model for the iron pole with the same variance as in the paper [1]was applied. Due to the used Stroud formulas, the same distribution had to be assumed with a relatively high variance based on [7] for the reluctivity of a PM. The last parameter was rather of "the mathematical relevance" and simulates the high impact of the air-gap parameters into the electromagnetic torque [6].

by using a multi-dimensional quadrature rule with corresponding weights w_k

$$\mathrm{v}_i(\mathbf{x}) := \langle \mathrm{A}(\mathbf{x}, \boldsymbol{\upsilon}), \Phi_i(\boldsymbol{\upsilon}) \rangle \approx \sum_{k=0}^{K} w_k \mathrm{A}\left(\mathbf{x}, \boldsymbol{\upsilon}^{(k)}\right) \Phi_i(\boldsymbol{\upsilon}^{(k)}). \tag{8}$$

4 Multi-level set representation

The level set method, first proposed in [12], has recently found a wide application in electrical engineering to address the design, shape and topology optimization problems, see e.g. [5, 14]. To trace the two interfaces between different materials with some assumed variations such as air, iron and PM poles of rotor, the modified multilevel set method (MLSM) has been used [13, 15]. Thus, we extend this framework into the situation, where the material parameter exhibit some uncertainty. These domains are described using two signed distance functions

$$\begin{aligned} &\mathrm{D}_1 = \{\mathbf{x} \in \mathrm{D} | \phi_1 > 0 \text{ and } \phi_2 > 0\}, \quad \mathrm{D}_2 = \{\mathbf{x} \in \mathrm{D} | \phi_1 > 0 \text{ and } \phi_2 < 0\}, \\ &\mathrm{D}_3 = \{\mathbf{x} \in \mathrm{D} | \phi_1 < 0 \text{ and } \phi_2 > 0\}, \quad \mathrm{D}_4 = \{\mathbf{x} \in \mathrm{D} | \phi_1 < 0 \text{ and } \phi_2 < 0\}, \end{aligned} \tag{9}$$

with $\phi(x)$ a signed distance function that is shown on Fig. 2.[2] In this situation, the reluctivity υ and the remanent flux density coefficient b_r (of the PM-material) read

$$\begin{aligned} \upsilon(\boldsymbol{\phi}, \boldsymbol{\xi}) = {} & \upsilon_1(\xi_1) H(\phi_1) H(\phi_2) + \upsilon_2(\xi_2) H(\phi_1)(1 - H(\phi_2)) + \\ & + \upsilon_3(\xi_3)(1 - H(\phi_1)) H(\phi_2) + \upsilon_4(\xi_4)(1 - H(\phi_1))(1 - H(\phi_2)), \end{aligned} \tag{10}$$

$$\begin{aligned} b_r(\boldsymbol{\phi}) = {} & b_{r1}(H(\phi_1) H(\phi_2) + b_{r2}(H(\phi_1)(1 - H(\phi_2)) + \\ & + b_{r3}((1 - H(\phi_1)) H(\phi_2) + b_{r4}(1 - H(\phi_1))(1 - H(\phi_2)) \end{aligned} \tag{11}$$

with $H(\cdot)$ the Heaviside function. The evolution of ϕ_i is described by the Hamilton-

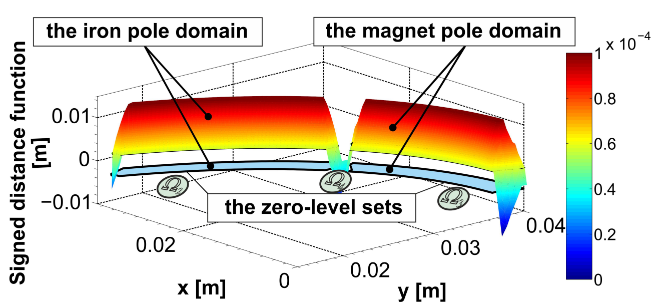

Fig. 2 Distribution of the signed distance function.

Jacobi-type equation [12] (during optimization with pseudo-time t)

[2] Notice, D_4 is an auxilliary set. We need in our application D_1, D_2, D_3, only.

$$\frac{\partial \phi_i}{\partial t} = -\nabla \phi_i (\mathbf{x}, t) \frac{d\mathbf{x}}{dt} = V_{n,i} |\nabla \phi_i|, \qquad (12)$$

where $V_{n,i}$ is the normal component of the zero-level set velocity corresponding to the objective function (14) and the forward problem (4). Fig. 2 shows the exemplary the distance function in fifth iteration of the optimized process, where shapes of rotors poles (the blue shape with black lines) is described by the zero-level set.

5 Robust topology optimization problem

The cogging torque minimization in the 2-D magnetostatic setting can be equivalently formulated as minimization of the magnetic energy W_r variation [15,16]. The advantage of the latter formulation is the calculation of the sensitivity in efficient way as follows [16]:

$$\frac{\partial W_\mathrm{r}}{\partial \mathbf{p}} = \int_\gamma (\upsilon_1 - \upsilon_2) \mathbf{B}_1 \cdot \mathbf{B}_2 - (\mathbf{M}_1 - \mathbf{M}_2) \cdot \mathbf{B}_2 \mathrm{d}\gamma, \qquad \text{in D.}, \qquad (13)$$

with υ_1 and υ_2 the reluctivities for different domains. Since the energy operator is self-adjoint, the dual and primary problem are the same. However, for the shape optimization problem constrained by the elliptic PDEs (4) with random material variations, the magnetic energy is defined as

$$W_\mathrm{r}(\upsilon(\phi_1, \phi_2, \xi)) = \int_\mathrm{D} \mathbf{B}(\phi_1, \phi_2) \mathbf{H}(\phi_1, \phi_2) \mathrm{d}\mathbf{x} + \sum_{i=0}^{I} \beta_i TV(\phi_i), \qquad (14)$$

which is subjected to the constraint (3) with $\mathbf{B}_r$ replaced by $\mathbf{B}_r(\phi_1, \phi_2)$[3] and $\mathbf{B}(\phi_1, \phi_2)$, while the $TV()$ denotes the Total Variation regularization with the coefficients β_i that account for controlling the geometrical complexity of obtained shapes [15] . Finally, this constraint has been introduced approximately to the optimization problem as two area constraints (for each rotor pole separately), which are involved in the level set method scheme, see, e.g., [14, 15]. Furthermore, we formulate the optimal shape optimization in the framework of the robust optimization [17] using the statistical moments such as the expectation and the standard deviation

$$\begin{aligned} \min_{\boldsymbol{\phi}} &: \mathrm{E}[W_\mathrm{r}(\boldsymbol{\upsilon})] + \kappa_1 \sqrt{\mathrm{Var}[W_\mathrm{r}(\boldsymbol{\upsilon})]} \\ \text{s.t.} &: \mathbf{K}\left(\boldsymbol{\upsilon}^k\right) \mathbf{A}^k = \mathbf{f}^k,\ k = 0, ..., K, \\ & \quad \upsilon_{\max j} \leq \upsilon_j \leq \upsilon_{\min j},\ j = 1, 2, \end{aligned} \qquad (15)$$

where κ_1 is a prescribed parameter, $\mathbf{K}$ denotes the stiffness matrix (at $K+1$ quadrature grid points). In this case, it is possible to calculate the total derivative of the

[3] To avoid to impose explicitly the constraints related to B_r two area constraint for each rotor poles separately as in work by [15] : $G_1(\phi) = |D_\mathrm{FE}|/|D_{\mathrm{FE}_0}| - S_\mathrm{FE} = 0$ and $G_2(\phi) = |D_\mathrm{PM}|/|D_{\mathrm{PM}_0}| - S_\mathrm{PM} = 0$ with the prescribed coefficients S_FE and S_PM were introduced.

function eq. (14) based on only the analysis of the forward model in the collocation points and taking eqs. (10), (11) and (13) and then (8), (7) into account. The similar approach, but for different type of the functional was used in [**?**] for the solution of stochastic identification/control problems for constrained PDEs with random input data.

6 Numerical results

The procedure described in the previous section has been applied to design the rotor poles of the ECPSM for no-load state (the excitation current is $J = 0$). The main parameters of the machine are given in Table 1. The initial configuration of the ECPS machine is depicted in Fig 3 (left). The quantities that are taken subject to variations are the reluctivity of the iron pole and the PM pole. Also the reluctivity of the air-gap is assumed to be uncertain. To model the uncertainty, we choose a uniform distribution of the reluctivity with a maximum deviation from a nominal value $\upsilon_{\mathrm{N}}(\mathbf{x}, |\nabla\mathbf{A}|^{\mathbf{2}})$ of 10%. The application of Stroud-5 points for a system of the ECPSM machine with three parameters yields $K = 19$ sample points $\{\boldsymbol{\xi}_i\}_{i=0}^{18}$ in the three-dimensional parameter space. The optimized rotor poles are shown in Fig. 3 (right).[4] For the optimal configuration the CT is calculated over a half of the period

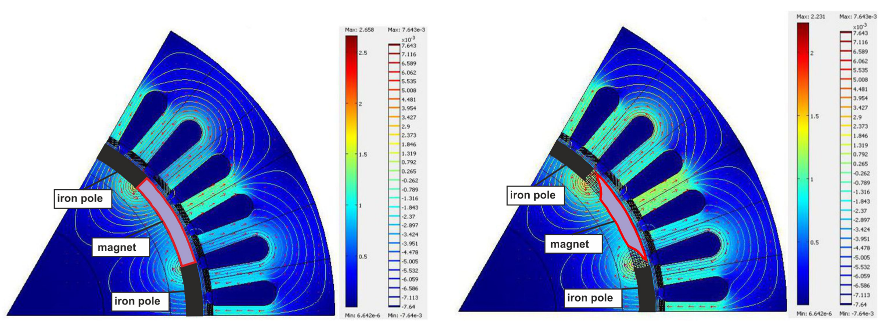

Fig. 3 Topology of the ECPSM: initial (left), optimal (right)

to assess the stator teeth interaction with the rotor poles, shown in Fig. 4 (left). The pick value of the CT expected value is reduced around 75%.

[4] The construction of a PM machine under consideration was a topic of the scientific project called *"The Electrically Controlled Permanent Magnet Excited Synchronous Machine (ECPSM) with application to electro-mobiles"* under the Grant No. N510 508040, where among others a small prototype of the deterministically optimized machine with the similar topology as obtained in our paper was investigated.

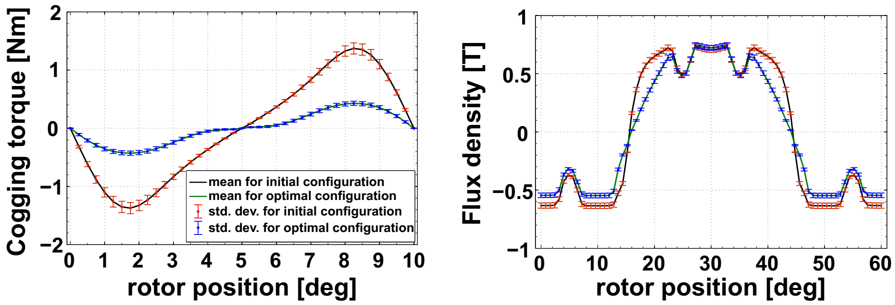

Fig. 4 Mean and standard deviation for initial and optimized topology of the ECPSM: Cogging torque (left), Flux density (right).

7 Conclusion

This paper demonstrated the incorporation of the SCM into the MLSM for the robust topology optimization of a PM synchronous machine. For this purpose, the shape of rotor poles was investigated. This methodology resulted in the minimization of the level of noise and vibrations by the significant reduction both the rectified) mean of the CT (70%) and standard deviation, while taking the manufacturing tolerances/variations into account. This work also highlights the effectiveness of the proposed methodology.

Acknowledgements The project nanoCOPS (Nanoelectronic COupled Problems Solutions) is supported by the European Union in the FP7-ICT-2013-11 Program under the grant agreement number 619166 and the SIMURON project is supported by the German Federal Ministry of Education and Research (05M13PXB).

References

1. A. Bartel , H. De Gersem, T. Hülsmann, U. Römer, S. Schöps, T. Weiland, Quantification of Uncertainty in the Field Quality of Magnets Originating from Material Measurements, *IEEE Transactions on Magnetics*, 49(5):2367-2317, 2013.
2. F. Gieras, and M. Wing, Permanent magnet motor technology, John Wiley & Sons Ltd., 2008.
3. Z. Makni, M. Besbes, and C. Marchand, Multiphysics Design Methodology of Permanent-Magnet Synchronous Motors, *IEEE Trans on Vehic. Techn.*, 56(4):1524–1530, 2007.
4. M.S. Islam, R. Islam, and T. Sebastian, Experimental verification of design techniques of permanent-magnet synchronous motors for low-torque-ripple applications, *IEEE Trans. Ind. Appl.*, 47(1):88–95, 2011.
5. P. Putek, P. Paplicki, and R. Palka. Low Cogging Torque Design of Permanent Magnet Machine Using Modified Multi-Level Set Method With Total Variation Regularization, *IEEE Trans.Magn.*, 50:657–660, 2014.
6. P. Sergeant, G. Crevecoeur, L. Dupré and A. van den Bossche, Characterization and optimization of a permanent magnet synchronous machine. *COMPEL*, 28:272–284, 2008.
7. J.M.M. Rovers, J. W. Jansen, and E. A. Lomonova. Modeling of Relative Permeability of Permanent Magnet Material Using Magnetic Surface Charges, *IEEE Trans.Magn.*, 49:2013–2919, 2013.

8. R. Pulch, Stochastic collocation and stochastic Galerkin methods for linear differential algebraic equations, *Journal of Computational and Applied Mathematics*, 262:281–291, 2014.
9. D. Xiu and J.S. Hesthaven, High-Order Collocation Methods for Differential Equations with Random Inputs,*SIAM J. Sci. Comput.*, 27(3):11181139, 2005.
10. A.H. Stroud, Some fifth degree integration formulas for symmetric regions *Mathematics of Computation*, 20(93):90–97, 1966.
11. D. Xiu, Numerical methods for stochastic computations: a spectral method approach, Princeton University Press, 2010.
12. S.J. Osher, J.A. Sethian, Fronts propagating with curvature dependent speed: algorithms based on Hamilton-Jacobi formulations, *J. Comput. Phys.* 79:12–49, 1988.
13. L.A. Vese and T.F. Chan, A multiphase level set framework for image segmentation using the Mumford and Shah model, *Int. J. Comput. Vis.*, 50(3):271–293, 2002.
14. S. Lim, S. Min, and J.P. Hong, Low torque ripple rotor design of the interior permanent magnet motor using the multi-phase level-set and phase-field concept, *IEEE Trans. on Magn.* 48(2):907–909 2012.
15. P. Putek, P. Paplicki, and R. Palka. Topology optimization of rotor poles in a permanent-magnet machine using level set method and continuum design sensitivity analysis, *COMPEL*, 66:1-21, 2014.
16. D. Kim, J. Sykulski, and D. Lowther, The implications of the use of composite materials in electromagnetic device topology and shape optimization, *IEEE Trans. on Magn.*, 45:1154–1156, 2009.
17. W. Yao, X. Chen, W. Luo, M. van Tooren, and J. Guo, Review of uncertainty-based multidisciplinary design optimization methods for aerospace vehicles, *Progress in Aerospace Sciences*, 47:450–479 (2011).
18. H. Tiesler, R.M. Kirby, D. Xiu, and T. Preusser, Stochastic collocation for optimal control problems with stochastic PDE constraints, *SIAM J. Numer. Anal.*, 50:2659–2682 (2012).